Design, fabrication, and measurement of frequency-selective surfaces

Maurizio Bozzi
Luca Perregrini
Department of Electronics
University of Pavia
Via Ferrata 1
I-27100 Pavia, Italy
E-mail: m.bozzi@ele.unipv.it

Jochen Weinzierl
Laboratories for High Frequency Technology (LHFT)
University of Erlangen-Nürnberg
Cauerstrasse 9
D-91058 Erlangen, Germany

Carsten Winnewisser
Freiburg Materials Research Center
University of Freiburg
Stefan-Meier-Strasse 21
D-79104 Freiburg, Germany

Abstract. This paper describes theoretical analysis, fabrication techniques, and measurement results for frequency-selective surfaces operating in the millimeter and submillimeter wave region. The analysis is based on the method of moments with entire domain basis functions, obtained by the boundary-integral–resonant-mode-expansion method. This method is particularly efficient and applies to the analysis of thick metal screens perforated periodically with arbitrarily shaped apertures. Three fabrication techniques are discussed and applied: photolithographic etching, galvanizing growth, and milling. Prototypes obtained with the different fabrication techniques are presented. Finally, measurements of the frequency response of the prototypes are presented, based on a new spectroscopic tool called terahertz time-domain spectroscopy. In all cases, the measurement data fit very well with the simulations.
 [S0091-3286(00)03308-0]

Subject terms: frequency-selective surfaces; method of moments; entire domain basis functions; photolithographic etching; galvanizing growth; milling technique; terahertz time-domain spectroscopy (THz-TDS).

Paper 990483 received Dec. 16, 1999; revised manuscript received Feb. 17, 2000; accepted for publication Feb. 17, 2000.

1 Introduction

Metal screens perforated periodically with apertures of various shapes are widely used as frequency-selective surfaces (FSSs) (or frequency-selective components, FSCs) in the millimeter and submillimeter wave range (Fig. 1).[1,2] The shape of the apertures, their size and spacing, and the thickness of the metal screen determine the frequency behavior of the FSS. These components find various applications as filters,[3,4] in quasioptical frequency multipliers,[5] in diplexing applications,[6] in laser cavities,[7] and in Fabry-Perot interferometers.[8] This paper covers three different topics related to the realization of FSSs: design, fabrication technologies, and measurement techniques.

Many numerical methods have been applied to the analysis of FSSs: the most popular are the finite-difference time-domain (FDTD) method,[9] the finite-element method (FEM),[10] and the integral-equation method (IEM).[11] The FDTD method and the FEM apply to arbitrary structures, but typically are quite slow. Conversely, the IEM is very efficient if used with entire domain basis functions, whose application, however, is usually limited to particular shapes.[12] On the other hand, subdomain basis functions (e.g., rooftops) have been typically used in the analysis of arbitrarily shaped apertures, leading to long CPU time and large memory requirement.[13] Recently, we have overcome this drawback by using (also in the case of arbitrarily shaped apertures) entire domain basis functions,[14,15] obtained by the boundary-integral–resonant-mode-expansion (BI-RME) method.[16–18] This approach resulted in a fast and flexible computer code, which performs the wideband analysis of FSSs with arbitrarily shaped apertures in tens of seconds on a standard PC. This code is so designed that it can be effectively embedded in a CAD tool for the analysis and optimization of FSSs.

An accurate fabrication technique is also required. Among the available techniques for the fabrication of FSSs in the millimeter and submillimeter wavelength range, we consider in this work both photolithographic and micromechanical approaches. Photolithographic techniques are used to fabricate printed FSSs, which comprise a periodic array of apertures in a thin conductive screen, either backed by a dielectric substrate or freestanding.[19] In this paper, we compare two photolithographic techniques we applied for the realization of printed FSSs. In the first method, we used a photolithographic etching process on a commercially available thin copper foil for the structuring of the FSS. This process is compared with the second method we used, which is based on a galvanizing growth on a base substrate, where we managed to directly fabricate the free-standing perforated copper foil. Besides these photolithographic techniques, we present also a mechanical technique, which permits producing perforated thick metal plates, acting as high-pass filters.[20] These filters are compact and physically robust.

Transmission measurements of FSSs, especially in the terahertz region, require sophisticated techniques. In the past decade spectroscopic techniques in the millimeter and the submillimeter wave region have been expanded by a new spectroscopic tool called terahertz time-domain spectroscopy (THz-TDS).[21] THz-TDS allows broadband measurements in the terahertz region, which is difficult to access by conventional techniques like microwave and Fourier transform spectroscopy. THz-TDS has proved to be a powerful tool for fast characterization of FIR properties of objects as diverse as gases,[21,22] dielectrics,

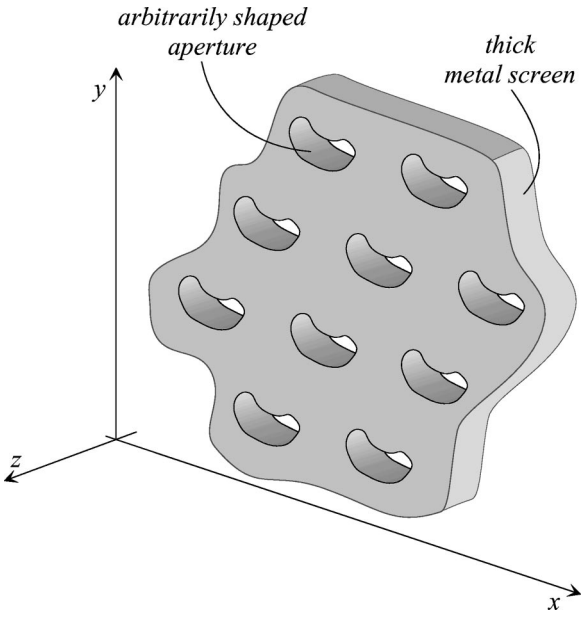

Fig. 1 A frequency-selective surface with arbitrarily shaped apertures.

semiconductors,[23] superconductors,[24] liquids,[25] flames,[26] and frequency-selective surfaces.[27] For this reason, we used the THz-TDS technique to characterize the frequency response of FSSs operating in the terahertz region: Sec. 4 outlines the basics of this technique and describes our measurement setup.

The analysis of FSSs by the BI-RME method, the different techniques used in the fabrication, and the measurements by the THz-TDS method are extensively discussed in this paper. Many experimental results are reported.

2 Theoretical Analysis of FSSs

The proposed theoretical approach permits us to calculate the frequency response of FSSs consisting of thick metal screens, perforated periodically with apertures of arbitrary shape (Fig. 1), and illuminated by a uniform plane wave. This algorithm was first presented in Ref. 14 for the analysis of infinitely thin perforated screens and was extended to the case of thick screens in Ref. 15.

Due to the periodicity of the structure, we apply the Floquet theorem,[28] and the analysis reduces to the investigation of a single unit cell (Fig. 2). By using the equivalence theorem, the two apertures connecting the waveguide section with free space are closed by perfectly conducting walls, and (unknown) magnetic current densities are defined over the surfaces of the apertures. Thus, the region of interest is split into three parts: the free space on the two sides of the metal screen, and the waveguide section (see Fig. 2). The aim of the analysis is the determination of the unknown magnetic currents, which allow for determining the transmitted and reflected fields. To this end, the continuity of the tangential components of the fields is enforced across the interfaces between the three regions. The resulting integral equation is solved by using the method of moments (MoM) in the Galerkin form. The unknown magnetic currents are expressed as a weighted summation of entire domain basis functions, which are the electric modal fields

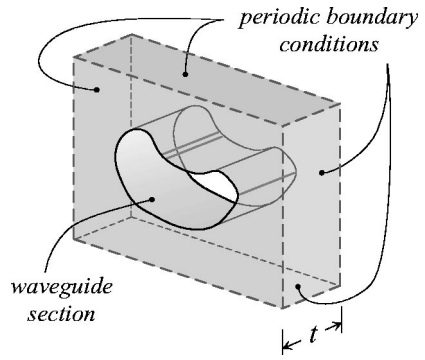

Fig. 2 The unit cell of the frequency-selective surface.

of the waveguide. Moreover, the fields in free space are expressed as a combination of Floquet modes, whereas the fields in the waveguide are represented as a combination of the modal fields of the waveguide.

The entire domain basis functions are numerically determined in a very efficient way by using the BI-RME method.[16] This method is very fast and flexible; it allows calculating a large number of modes of an arbitrarily shaped waveguide in a few seconds. Furthermore, the method yields as a primary result the boundary values of the potentials of the TE and TM waveguide modes. These results can be used for a direct calculation of the integrals involved in the MoM matrices, by reducing surface integrals to line integrals.[14]

The possibility of considering arbitrarily shaped apertures has a tremendous relevance. In fact, it allows for taking into account the unavoidable inaccuracies due to the fabrication process, e.g., rounding of edges or corners in the aperture shape. This issue is extensively discussed in Sec. 3. Moreover, the experimental results reported in Sec. 5 outline features of our code that are of paramount importance in achieving very accurate results.

3 Fabrication Process

In this section, our experience in the use of different techniques for the fabrication of FSSs in the millimeter and submillimeter wave region is presented, showing that some techniques guarantee good accuracy in the aperture pattern.

We started the FSS fabrication with a photolithographic etching process. A commercially available copper foil with a thickness of 30 μm was mounted on a frame to avoid damage during the numerous fabrication steps. This foil was covered with photoresist, and after the exposure and development of the resist, the etching process was started. Due to underetching effects, the reproduction of the contour of the small apertures in the etched copper foil was extremely bad. Especially in the case of bandpass filters for frequencies higher than 200 GHz (where the aperture size is very small), the contour of the apertures in the copper foil was strongly deformed. A fabrication example of a quasioptical bandpass filter with cross-shaped apertures for 435-GHz center frequency is shown in Fig. 3; the cross shape can hardly be recognized.

Due to the bad results of the etching process, we decided to use a galvanizing growth process to avoid the underetching problem. The foils are grown on a base substrate made

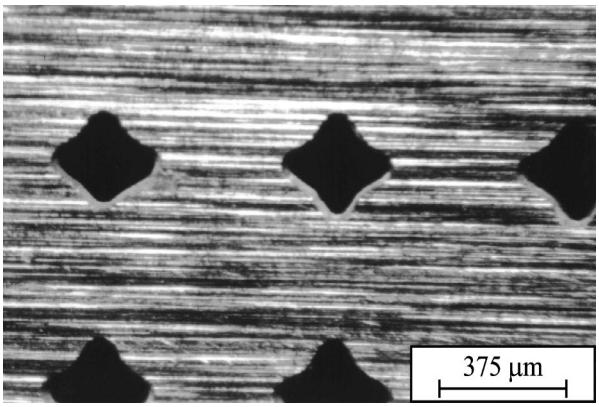

Fig. 3 Photograph of an etched bandpass filter for 435-GHz center frequency. The contour of the cross-shaped apertures can hardly be recognized, showing the unsuitability of the etching fabrication technique in this frequency range.

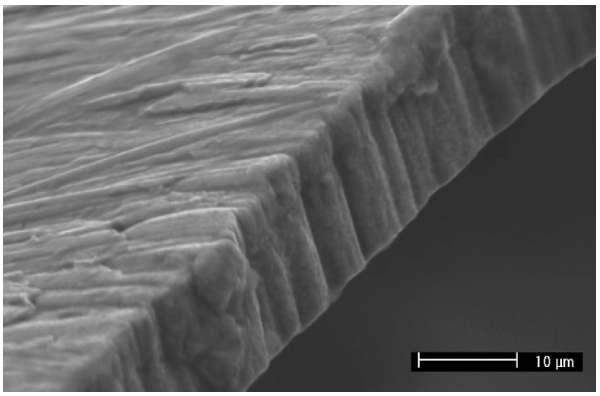

Fig. 5 Microscope photograph of a resonator edge of a galvanized band-pass filter.

of copper, which is partly covered with photoresist according to the outline of the filter apertures. In order to get sufficient mechanical stability of the foils, a thickness of minimum 6 μm of the grown copper layer had to be realized. Therefore we used a fixed photoresist with a thickness of 25 μm. The last step in this galvanizing fabrication process is the nondestructive removal of the grown copper foil from the substrate, which is a very critical step. We solved this problem by using an aluminum oxide coating on the copper substrate, which reduces the adhesion of the grown copper layer to the base substrate so that the perforated copper foils can be removed from the substrate without any damage. Figure 4 shows a photograph of a galvanized freestanding 280-GHz mesh filter.[19]

The high accuracy of the galvanizing growth procedure due to the avoidance of underetching can be observed. In Fig. 5 a microscope photograph of a resonator edge of a galvanized filter shows the sharp micro outline.

Additionally, we measured the surface roughness using a perthometer. The average roughness of the galvanized foils was lower than 1 μm, but it gives rise to small additional ohmic losses. With this fabrication technique we realized the described mesh filters for center frequencies up to 1 THz.

A different technique was adopted for the fabrication of dichroic filters, consisting of thick metal screens perforated with an equilateral array of hexagonally close-packed circular holes. These filters have been used in the millimeter wavelength region for a long time and have been scaled down into the submillimeter region by the use of numerically controlled milling machines.[27] They provide a sharp frequency response, which is achieved when the thickness t of the metal plate, the hole diameter d, and the spacing s (see Fig. 6) have a ratio of approximately 1:1.2:1.6.[27,29] This mechanical technique is limited by its nature to circular apertures with minimum hole diameters due to the finite size of feasible drills. Therefore, limitations are encountered in fabricating dichroic plates with cutoff frequency above $\approx$2 THz. In this frequency range the thickness of the metal plate is below $\approx$70 μm, allowing the consideration of other fabrication processes like photolithography, galvanizing growth, or even laser ablation.

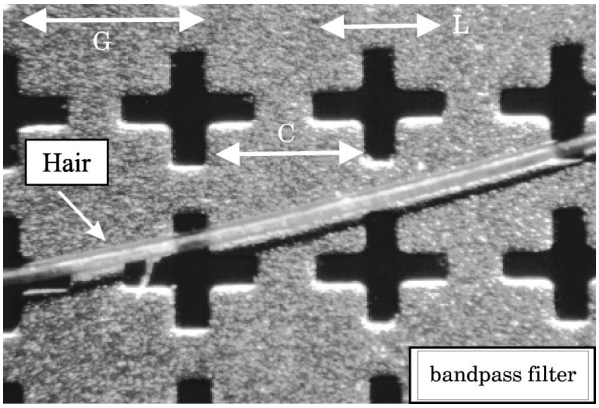

Fig. 4 Microscope image of a galvanized cross-shaped bandpass filter with a resonance frequency of 280 GHz. The parameter set of the cross-shaped apertures is: mesh period $G=810$ μm, slot length $L=570$ μm, strap width $C=650$ μm, and foil thickness $t=10$ μm.

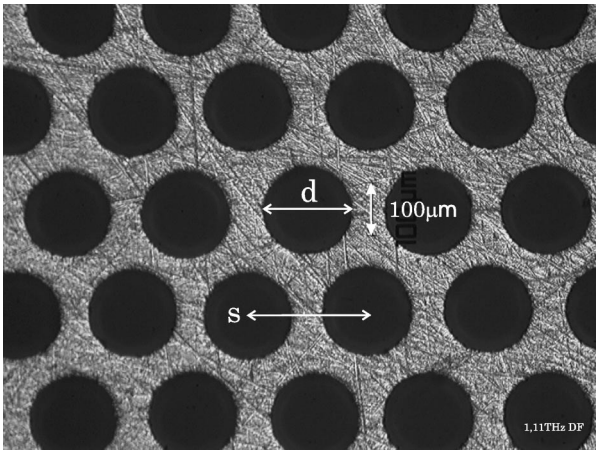

Fig. 6 Microscope image of a segment of a dichroic filter with a cutoff frequency at 1.11 THz. The material consists of a brass plate ($t=153$ μm) with holes ($d=168$ μm) drilled by numerically controlled milling machine in a hexagonal array ($s=226$ μm).

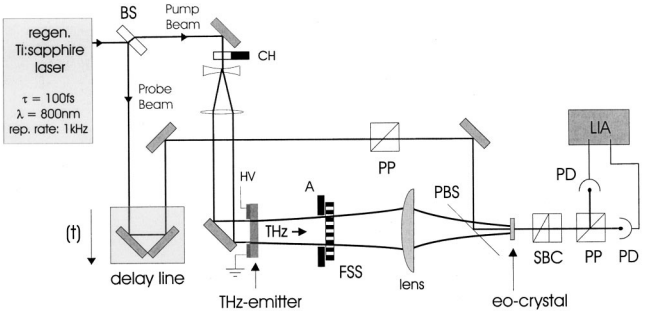

Fig. 7 Setup of the terahertz time-domain spectrometer: BS: beamsplitter; CH: chopper; THz-emitter: large aperture ($\approx 1\ \mathrm{cm}^2$) antenna; HV: applied high voltage; FSS: frequency-selective surface; lens: high-density polyethylene lens; PP: polarizing prisms; PBS: pellicle beamsplitter; eo-crystal: ZnTe crystal; SBC: Soleil-Babinet compensator; PD: balanced photodiodes; LIA: lock-in amplifier.

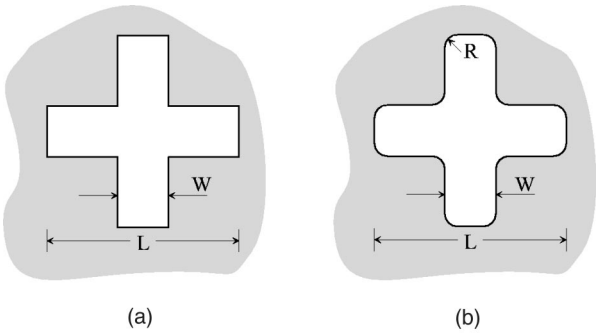

Fig. 8 Geometry of the aperture of the cross-shaped filter: (a) the cross with sharp corners; (b) the cross with rounded corners. The dimensions of the aperture are: $L=570\ \mu$m, $W=160\ \mu$m, $R=40\ \mu$m; the spacing between the apertures is 810 μm.

4 Measurement Technique

THz-TDS is based on the excitation of biased semiconductors or electro-optic crystals by a femtosecond laser pulse. In the case of a biased photoconducting material, here GaAs, a transient current gives rise to the emission of an electromagnetic (EM) pulse of typically less than 1-ps time duration. This EM (terahertz) pulse comprises a frequency spectrum ranging from a few gigahertz up to the terahertz region. In the case of an electro-optic crystal, optical rectification of the femtosecond laser pulse generates the terahertz pulse.[30] Optical sampling permits coherent detection of the electric field strength of the terahertz pulse, thus enabling the measurement of both the real and imaginary parts of the dielectric function of materials.

In our measurement setup, the filter transmission characteristics have been measured with an electro-optic (EO) sampling terahertz time-domain spectrometer, shown in Fig. 7. Pulses from a regenerative Ti:sapphire oscillator are divided by a beamsplitter into a probe and a pump beam. The latter illuminates a GaAs wafer to generate the terahertz pulse, which is linearly polarized parallel to the applied high voltage. The detection setup, consisting of an EO crystal between a pair of crossed polarizers, can be referred to as an ultrafast transverse EO modulator, which allows one to detect the electric field strength of the terahertz pulse as an intensity variation of the optical probe pulse. The temporal shape of the terahertz pulse, $E(t)$, is recorded by varying the delay line of the optical probe pulse. The FSS is placed halfway between the terahertz emitter and the high-density polyethylene lens, and the terahertz pulse reaches the FSS after 9 cm of free-space propagation at normal incidence as a plane wave.[31] For further details on the measurement setup the reader is referred to Ref. 32.

The electric field strength of the terahertz pulse, $E(t)$, is recorded with and without the FSS placed in the path of the terahertz beam. By taking the Fourier transform of the time-domain data $E(t)$, one obtains the complex amplitude spectrum $\tilde{E}(\nu)$ in the form of both magnitude $E(\nu)$ and phase $\phi(\nu)$. The power transmittance $T_P(\nu)$ is obtained by taking the square of the ratio between the Fourier-transformed sample and reference data:

$$T_P(\nu)=\left[\frac{E_{\mathrm{sample}}(\nu)}{E_{\mathrm{ref}}(\nu)}\right]^2. \tag{1}$$

An electromagnetic wave transiting an FSS encounters a phase shift of

$$\Delta\phi(\nu)=\phi_{\mathrm{sample}}(\nu)-\phi_{\mathrm{ref}}(\nu). \tag{2}$$

5 Numerical and Experimental Results

In this section, we compare some theoretical analyses performed with the method described in Sec. 2 to the measurement data.

The first example refers to the cross-shaped bandpass filter shown in Fig. 4. The dimensions of the cross aperture are reported in Fig. 8(a). The thickness of the metal screen is $t=10\ \mu$m, and the incident field is a vertically polarized uniform plane wave, incident from the normal direction.

In the first analysis, we calculated the power transmittance and the phase shift of the filter in the frequency range 10 to 1500 GHz. In this simulation, we used 26 entire domain basis functions, i.e., waveguide modes, and 425 Floquet modes. The overall computing time on a PC Pentium II (200 MHz) was 86 s for the calculation of the frequency response at 150 frequency points. It is worth noting that the calculation of the waveguide mode spectrum (i.e., the set of entire domain basis functions) required only 10 s.

Figure 9 shows the power transmittance and the phase shift versus the frequency: the results obtained with our numerical code are compared with the measurement data. We observe good agreement between theory and measurements, except for a small shift of the resonance frequency, which is 11 GHz lower than expected. This frequency shift is due to the unavoidable smoothness of the aperture boundary, resulting from the fabrication process. From the microscope photographs (see Fig. 4), it is possible to deduce that an arc of radius $R=40\ \mu$m should be considered instead of the sharp corners. On considering the smoothed cross [Fig. 8(b)], the calculated resonance frequency of the filter shifts upward, getting closer to the measured one (Fig. 10). The results of the analysis of the smoothed cross are in excellent agreement with the measurement data over the whole frequency band. Due to the flexibility of our code,

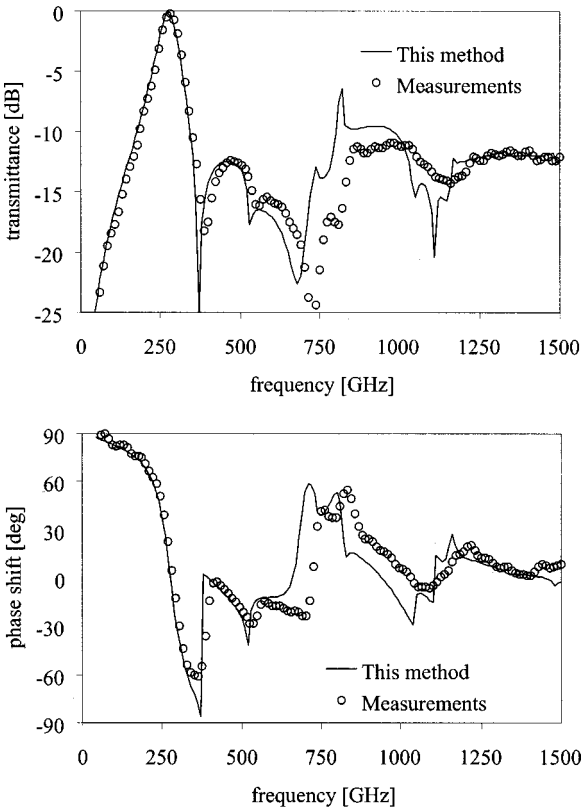

Fig. 9 Numerical results for the filter considering the aperture shape with sharp corners [Fig. 8(a)], compared with experimental data. The transmittance phase is the difference between the phase measured with and without the filter.

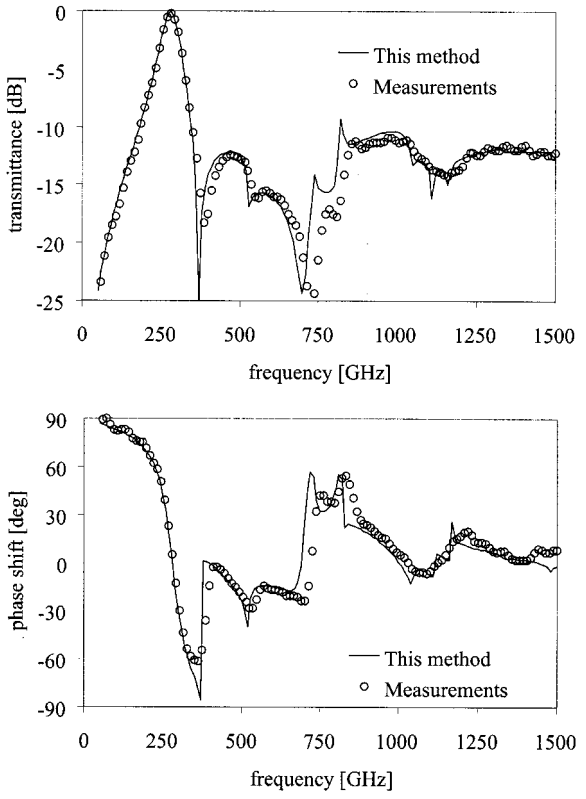

Fig. 10 Numerical results for the filter considering the aperture shape with rounded corners [Fig. 8(b)], compared with experimental data.

Table 1 Characteristics of three dichroic filters fabricated by a CNC milling machine (see Fig. 6).

Filter	Hole spacing s (μm)	Hole diameter d (μm)	Metal thickness t (μm)	3-dB cutoff frequency (GHz)
D1	970	740	125	228
D2	970	740	700	242
D3	226	168	153	1112

the numbers of entire domain basis functions and of Floquet modes do not change; therefore the CPU time is unchanged.

The other three examples refer to dichroic filters with circular holes in a hexagonal array (Fig. 6), whose characteristics are given in Table 1. The measured and simulated transmittances and phase shifts of D1 and D2, which differ only in the thickness of the metal plate, are reported in Figs. 11 and 12. Also in these cases, the numerical results compare very well with the experimental ones, and the CPU time is very short: 58 s for the analysis of both D1 and D2 at 100 frequency points on a PC Pentium II (200 MHz). The main difference between D1 and D2 is the slope of the transition between the rejection band and the passband: as expected, the filter D2 (the thicker dichroic) exhibits a steeper transition across the cutoff frequency. This is mainly due to the fact that the longer the waveguide section (see Fig. 2), the higher the attenuation of the fundamental mode just below its cutoff frequency, and therefore the ter-

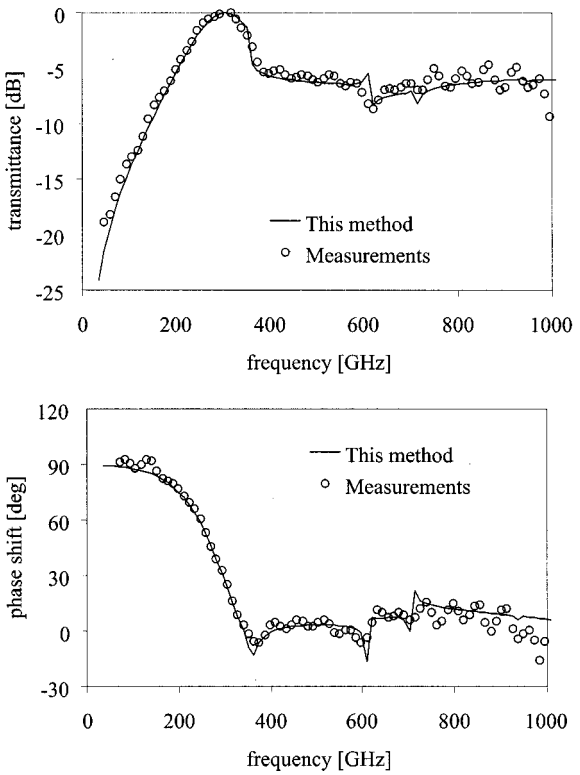

Fig. 11 Numerical results for the dichroic filter D1, compared with experimental data.

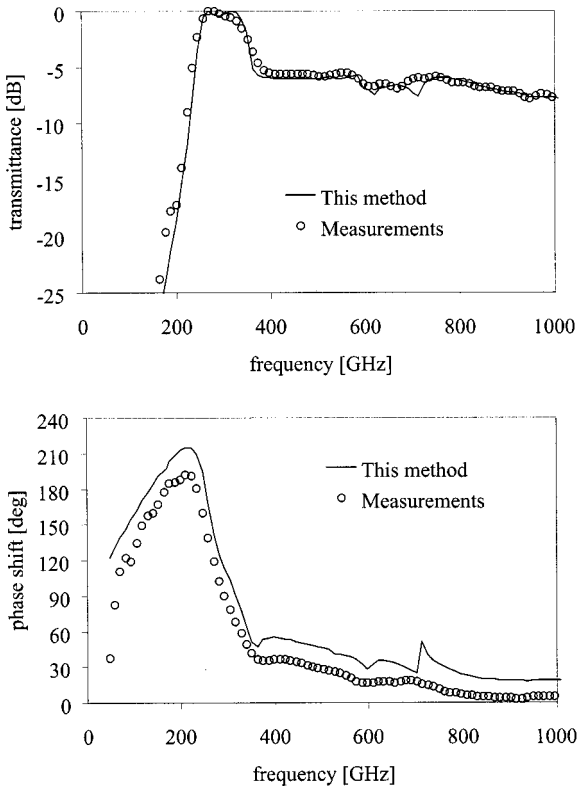

Fig. 12 Numerical results for the dichroic filter D2, compared with experimental data.

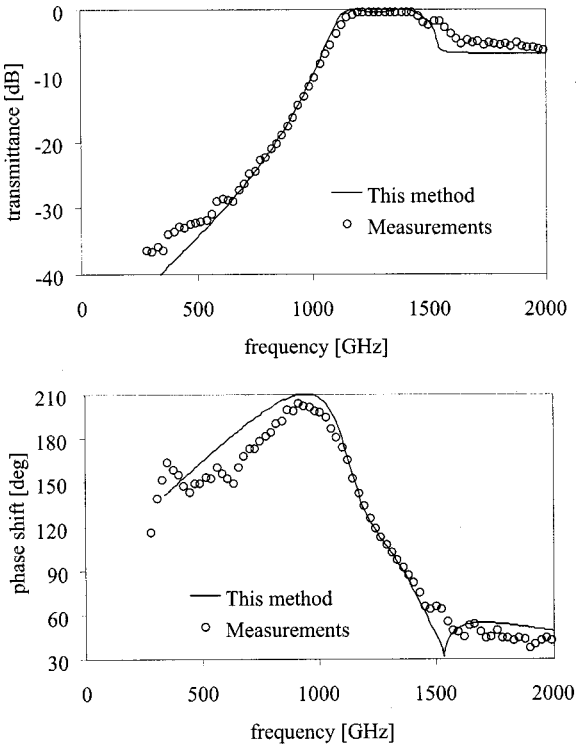

Fig. 13 Numerical results for the dichroic filter D3, compared with experimental data.

minal sections of the waveguide of D2 become rapidly uncoupled.

The dichroic D3 is very challenging, particularly for the mechanical structuring, since it is designed for operating with a cutoff frequency of 1.1 THz. Its frequency response, both measured and calculated, is reported in Fig. 13. The CPU time on a PC Pentium II (200 MHz) is 66 s for 200 frequency points. The good agreement between measured data and numerical results points out the effectiveness of the mechanical fabrication by CNC milling as well as the suitability of the measurement setup for high frequencies. More experimental interpretation of the transmittance characteristics, especially the phase-shift behavior, of dichroic filters can be found in Ref. 33.

6 Conclusions

In this paper we have discussed the fabrication of FSSs operating in the terahertz region, demonstrating its feasibility both by galvanizing growth and by mechanical (milling) machining. The frequency response of the prototypes was measured in the band 0 to 2 THz by a THz-TDS approach. The simulations, performed by a novel algorithm based on the BI-RME method, agree very well with the measurements.

Acknowledgment

This work was supported by the EU Commission under the TMR Program contract No. ERBFMRXCT960050 and by University of Pavia under F.A.R. Funding.

References

1. T. K. Wu, *Frequency Selective Surface and Grid Array*, Wiley (1995).
2. J. C. Vardaxoglou, *Frequency Selective Surfaces*, Wiley (1997).
3. R. Ulrich, ''Far-infrared properties of metallic mesh and its complementary structure,'' *Infrared Phys.* **7**, 37–55 (1967).
4. V. P. Tomaselli, D. C. Edewaard, P. Gillan, and K. D. Möller, ''Far-infrared bandpass filters form cross-shaped grids,'' *Appl. Opt.* **20**, 1361–1366 (1981).
5. F. Maiwald, F. Lewen, B. Vowinkel, W. Jabs, D. G. Paveljev, M. Winnewisser, and G. Winnewisser, ''Planar Schottky diode frequency-multiplier for molecular spectroscopy up to 1.3 THz,'' *IEEE Microwave Guid. Wave Lett.* **9**, 198–200 (1999).
6. C. Letrou and M. Gheudin, ''Dichroic diplexer design for millimeter waves,'' *Int. J. Infrared Millim. Waves* **13**, 27–42 (1992).
7. D. A. Weitz, W. J. Skocpol, and M. Tinkham, ''Capacitive-mesh output couplers for optically pumped far-infrared lasers,'' *Opt. Lett.* **3**, 13–15 (1978).
8. R. D. Rawcliffe and C. M. Randall, ''Metal mesh interference filters for the far infrared,'' *Appl. Opt.* **6**, 1353–1358 (1967).
9. P. Harms, R. Mittra, and Ko Wai, ''Implementation of the periodic boundary condition in the finite-difference time-domain algorithm for FSS structures,'' *IEEE Trans. Antennas Propag.* **42**(9), 1317–1324 (1994).
10. M. Lambea, M. A. Gonzalez, J. A. Encinar, and J. Zapata, ''Analysis of frequency selective surfaces with arbitrarily shaped apertures by finite element method and generalized scattering matrix,'' in *IEEE APS Int. Symp. 1995 Digest 3*, pp. 1644–1647 (1995).
11. T. F. Eibert, J. L. Volakis, D. R. Wilton, and D. R. Jackson, ''Hybrid FE/BI modeling of 3-D doubly periodic structures utilizing triangular prismatic elements and an MPIE formulation accelerated by the Ewald transformation,'' *IEEE Trans. Antennas Propag.* **47**(5), 843–850 (1999).
12. C. C. Chen, ''Transmission of microwave through perforated flat plates of finite thickness,'' *IEEE Trans. Microwave Theory Tech.* **21**(1), 1–6 (1973).
13. R. Mittra, C. H. Chan, and T. Cwik, ''Techniques for analyzing frequency selective surfaces—a review,'' *Proc. IEEE* **76**(12), 1593–1615 (1988).
14. M. Bozzi and L. Perregrini, ''Efficient analysis of thin conductive screens perforated periodically with arbitrarily shaped apertures,'' *Electron. Lett.* **35**(13), 1085–1087 (1999).
15. M. Bozzi, L. Perregrini, J. Weinzierl, and C. Winnewisser, ''Analysis of frequency selective surfaces for quasi-optical applications,'' in

Terahertz and Gigahertz Photonics, Proc. SPIE **3795**, 322–328 (1999).
16. G. Conciauro, M. Guglielmi, and R. Sorrentino, *Advanced Modal Analysis*, Wiley (1999).
17. G. Conciauro, P. Arcioni, M. Bressan, and L. Perregrini, ''Wideband modeling of arbitrarily shaped *H*-plane waveguide components by the 'boundary integral–resonant mode expansion method','' *IEEE Trans. Microwave Theory Tech.* **44**(7), 1057–1066 (1996).
18. P. Arcioni, M. Bressan, G. Conciauro, and L. Perregrini, ''Wideband modeling of arbitrarily shaped *E*-plane waveguide components by the 'boundary integral–resonant mode expansion method','' *IEEE Trans. Microwave Theory Tech.* **44**(11), 2083–2092 (1996).
19. D. Steup and J. Weinzierl, ''Resonant THz-meshes,'' in *Proc. 4th Int. THz Workshop*, Erlangen-Tennenlohe, Germany (1996).
20. L. A. Robinson, ''Electrical properties of metal-loaded radomes,'' Wright-Patterson Air Force Base, OH, Tech. Rep. WADD-TR-60-84, Nat. Tech. Info. Serv., U.S. Department of Commerce, Springfield, VA (1960).
21. M. van Exter, C. Fattinger, and D. Grischkowsky, ''Terahertz time-domain spectroscopy of water vapor,'' *Opt. Lett.* **14**, 1128–1130 (1989).
22. H. Harde and D. Grischkowsky, ''Coherent transients excited by subpicosecond pulses of terahertz radiation,'' *J. Opt. Soc. Am. B* **8**, 1642–1651 (1991).
23. D. Grischkowsky, S. Keiding, M. van Exter, and C. Fattinger, ''Far-infrared time-domain spectroscopy with terahertz beams of dielectrics and semiconductors,'' *J. Opt. Soc. Am. B* **7**(10), 2006 (1990).
24. M. C. Nuss, P. M. Mankiewich, M. L. O'Malley, E. H. Westerwichk, and P. B. Littlewood, ''Dynamic conductivity and coherence peak in YBaCuO superconductors,'' *Phys. Rev. Lett.* **66**, 3305–3308 (1991).
25. J. E. Pedersen and S. Keiding, ''THz time-domain spectroscopy of nonpolar liquids,'' *IEEE J. Quantum Electron.* **28**, 2518–2522 (1992).
26. R. A. Cheville and D. Grischkowsky, ''Observation of pure absorption spectra in the ν_2 band of hot H_2O in flames,'' *Opt. Lett.* **23**, 531 (1998).
27. C. Winnewisser, F. Lewen, J. Weinzierl, and H. Helm, ''Transmission features of frequency-selective components in the far infrared determined by terahertz time-domain spectroscopy,'' *Appl. Opt.* **38**, 3961–3967 (1999).
28. N. Amitay, V. Galindo, and C. P. Wu, *Theory and Analysis of Phased Array Antennas*, Wiley-Interscience, New York (1972).
29. J. W. Archer, ''A novel quasi-optical frequency multiplier design for millimeter and submillimeter wavelengths,'' *IEEE Trans. Microwave Theory Tech.* **32**, 421–426 (1984).
30. D. H. Auston and M. C. Nuss, ''Electrooptic generation and detection of femtosecond electrical transients,'' *IEEE J. Quantum Electron.* **24**, 184–197 (1988).
31. A. Gürtler, C. Winnewisser, H. Helm, and P. Uhd Jepsen, ''Terahertz pulse propagation in the near and far field,'' *J. Opt. Soc. Am. A* **17**(1), 74–83 (2000).
32. C. Winnewisser, F. Lewen, and H. Helm, ''Transmission characteristics of dichroic filters measured by THz time-domain spectroscopy,'' *Appl. Phys. A: Mater. Sci. Process.* **66A**, 593–598 (1998).
33. C. Winnewisser, F. Lewen, M. Schall, M. Walther, and H. Helm, ''Characterisation and application of dichroic filters in the 0.1 to 2 THz region,'' *IEEE Trans. Microwave Theory Tech.* **48**(4), 744–749 (2000).

Maurizio Bozzi received the Laurea degree in electronic engineering from the University of Pavia in October 1996. From December 1996 to September 1997 he was a guest researcher at the Technische Universität Darmstadt (Germany), in the framework of a European project (TMR) for the exchange of young researchers. Since November 1997 he has been a PhD Student at the Microwave Lab, University of Pavia. His main research activities concern the electromagnetic modeling of quasioptical circuits (frequency multipliers and frequency-selective surfaces) operating in the millimeter and submillimeter wave range. He is a student member of the IEEE.

Luca Perregrini received the Laurea degree in electronic engineering and the PhD from the University of Pavia in 1989 and 1993, respectively. In 1992, he joined the Department of Electronics of the University of Pavia as a researcher in electromagnetics, and he has been teaching a course in electromagnetic field theory since 1996. His current research interests are in numerical methods for the analysis and optimization of waveguide circuits, and in the electromagnetic modeling of quasioptical circuits (frequency multipliers and frequency-selective surfaces) in the millimeter and submillimeter wave range. Dr. Perregrini is a member of the IEEE.

Jochen Weinzierl received the DiplIng degree from the University Erlangen-Nürnberg, Germany, in 1996. Since 1996, he has been a PhD student at the Laboratories for High Frequency Technology in Erlangen. He is currently involved in a research project on a new multielement circuit technology for terahertz frequencies, supported by the German Research Council (DFG). His main research interests are the development of passive components for quasioptical circuits at terahertz frequencies as well as the development of complex field measurement systems in this frequency region.

Carsten Winnewisser received his diploma and PhD degrees in physics from the University of Freiburg, Germany in 1994 and 1999, respectively. From 1995 to 1999 he has been working on the generation, detection, and application of terahertz pulses in the Department of Molecular and Optical Physics. In 1997 he received a degree in medical physics and techniques from the University of Kaiserslautern, Germany. Presently he is working as a postdoctoral fellow at the Freiburg Materials Research Center of the University of Freiburg. His interests lie in luminescence conversion with LEDs and in the application of photonic structures in the far infrared and optical region. Dr. Winnewisser is a fellow of the German Physical Society (DPG).